Hierarchical Ordering of Quantum Dots and Liquid with Tunable Super-Periodicity into High Aspect Ratio Moiré Superlattice Structure

*Soo-Yeon Cho, Hwan-Jin Jeon, Jong-Seon Kim, Jong Min Ok, and Hee-Tae Jung**

In this work, a new approach for construction of high aspect ratio complex moiré superlattice structure with versatile super-periodicity is developed using the moiré fringe and secondary sputtering lithography. Wide assortments of high aspect ratio complex superstructures having different features on a 10 nm scaled wall are easily fabricated from simple starting components. More important is the finding of a new microscale phenomenon, consisting in trapping fluids in the centres of the moiré hexagonal fringes, as the consequence of the modulation of local hydrophilicty of the pattern. Using this phenomenon, target materials can be selectively and hierarchically confined within the moiré superlattice. Hierarchical nanoparticles (QDs) ordering with tunable super-periodicity into selective area of moiré superlattice are successfully demonstrated by just solution-casting of toluene based QD solution on patterned surfaces. This observation is expected to elucidate the key morphological factors that govern the physics of liquid behavior on a complex patterned substrate. Accordingly, in the near future, this facile approach for complex superlattice structure could be used as optical substrate for imaging applications and open interesting perspectives in the assembly processes and the handling of the nano-microsized particles.

1. Introduction

The development of complex lateral superlattice structures composed of nano-particles or nanopatterns has greatly enhanced the performance of a variety of nanotechnology and optoelectronic devices.[1–3] Recently, moiré fringes resulting from the mismatch between two lattices were shown to be a powerful tool for the generation of micro- and nanoscale complex superlattice structures.[4] These patterns, initially only of aesthetic interest, can now be fabricated easily onto a wide assortment of superstructures having various feature dimensions, through simple modification of the mismatch angles. A variety of methods, including both bottom-up and top-down approaches, have been developed for the fabrication of complex superlattice structures using the moiré fringe technique. Several bottom-up fabrication methods, which include block-copolymers,[4] DNA crystals,[5] polymer microparticles,[6] colloidal crystals,[7] and self-assembled nanorod arrays,[8,9] have been suggested for the formation of moiré superlattice structures. However, such soft-material-based moiré superlattice structures contain many defects and imperfections over a large area, limiting their potential application in areas such as plasmonic substrates,[10,11] hard templates for lithography,[4] and self-assembly.[12–14] On the contrary, top-down approaches such as nano-imprint lithography,[15] ion-beam lithography,[16] mechano-photopatterning,[17] and rotational-photolithography[18] produce a highly crystalline superstructure without defects and imperfections, and with high accuracy and reproducibility.

Despite considerable progress in this area, major challenges remain in the development of complex nano-scaled moiré patterns with multiple functions and multiple materials, and more research is required to greatly expand their application range. It is essential that the target materials for building up moiré patterns be diverse, from soft to hard materials, forming a robust superstructure. Having a diverse range of materials as candidates for forming moiré patterns can widen their range of application. In addition, complex superlattice structures having diverse functional properties should require only a simple fabrication method with high throughput, without needing complex process conditions or specialized optically sensitive materials.

In the study described below, we have developed a new procedure for the construction of multi-functional complex moiré superlattice structures, through an advanced secondary sputtering lithography (SSL) technique. The SSL technique developed by our group can achieve 10 nm scale nano-patterns through the secondary sputtering phenomenon during the ion-bombardment process.[19–22] A significant step was taken towards the realization of complex nano-scaled moiré superlattice structures, through the use of a multi-step SSL procedure. Along with control over the misorientation angle, we achieved highly periodic and high aspect ratio moiré superlattice

S.-Y. Cho, H.-J. Jeon, J.-S. Kim, J. M. Ok, Prof. H.-T. Jung
Department of Chemical
and Biomolecular Engineering
BK21+ program
Korea Advanced Institute of Science
and Technology (KAIST)
335 Gwahangno
Yuseong-gu, Daejeon 305–701, Korea
E-mail: heetae@kaist.ac.kr

DOI: 10.1002/adfm.201401981

structures over large areas. In addition, various complex moiré superlattice structures, including hole-cylindrical, ellipsoidal, and triangular shaped patterns, can be easily fabricated using a single pillar-shaped master pattern.[19,21,22]

Interestingly the resulting high aspect ratio complex moiré superlattice structures show a unique liquid trapping property: When a thin liquid layer was placed on the moiré substrate, the liquid droplet was selectively and periodically confined within the core of the hexagonal moiré superlattice, which has a relatively low pattern density. In addition, we demonstrate that high aspect ratio nano-scaled complex superstructures show intensive capillary forces on liquid droplets. Combining advantages of these two phenomena (moiré fringe and secondary sputtering phenomenon), we successfully demonstrate that nano particles (quantum dots (QDs)) can be selectively and periodically self-ordered into predetermined area of moiré superlattice structure. This unique substrate can potentially be used as optical substrates of imaging applications and plasmonic substrate while providing micron and sub-micron alignment ability.

This simple, rapid, and versatile superlattice fabrication process offers the potential for the production of multi-functional and multi-material structures with unique shapes. While difficult to achieve with previous lithographic techniques, this is made possible by the moiré fringe technique and SSL.

2. Result and Discussion

The schematic in **Figure 1** illustrates the process to fabricate a moiré superlattice structure with 10 nm walled hole-cylinder patterns using a double-step SSL technique. Firstly, the gold particles of the bottom gold layer (20 nm) were etched and emitted to the side surface of polystyrene (PS) pre-patterns with wide angle distribution, through the secondary sputtering phenomenon during the Ar ion-bombardment process[19] (Figure 1a). It is noteworthy to mention that while we used gold as the target material in this study, different types of metal or semiconductor moiré superlattice structures can be prepared, provided that different target layers are deposited onto a substrate.[19] Then, ≈400 nm thick PS films were spin-coated onto the patterned hexagonal shape of the hole-cylinder substrate with a ≈10 nm wall thickness resulting from the first SSL process (Figure 1b). The PS layer should be thick enough to cover the entire area of the pre-patterned hexagonal array. An identical PDMS mold to that used in the first SSL process was then pressed onto the PS surface at various misorientation angles (Figure 1c). The second PS pre-pattern was formed above the glass transition temperature (T_g) by capillary force within the hole-cylinder hexagonal array, and the residue was removed by the RIE process (Figure 1d). Finally, repeating the secondary sputtering phenomenon with the same procedure as in the first process, we can generate high aspect ratio moiré superlattice structures with complex nano hole-cylinder patterns (≈10 nm wall thickness). Because SSL pattern shows ultra-thin wall thickness (10 nm) and high aspect ratio (3) characteristics, the first SSL pattern didn't significantly etched out during anisotropic etching of second ion-milling process. As the degree of misorientation is varied from a small angle (Figure 1e) to a large angle (Figure 1f), hexagonal moiré superstructures with various feature dimensions and densities can be fabricated. As a result, complex superlattice structures having a broad range of periodicity can be prepared from a single pre-pattern by a combined SSL and moiré fringe technique. It is important to note that additional patterning processes (triple, quadruple, and multi-step processes) can be performed to fabricate more complicated superstructures.[22]

Figure 2a shows a representative scanning electron microscope (SEM) image of a high aspect ratio complex moiré superstructure on a glass substrate, revealing the formation of a highly ordered, periodic lateral superlattice over a large area (5 mm × 5 mm). The moiré pattern was formed by the double-step SSL process, in which the single hexagonal array underwent a secondary SSL process at a rotation angle of 15°. A fast Fourier transform (FFT) shows that the moiré superlattice consists of a single crystalline structure with an average hexagon periodicity of 3.5 μm (inset, left-bottom of Figure 2a). A magnified image shows novel nano-scale hole-cylinder arrangements with a periodically varying motif distribution (inset, top-right of Figure 2a). In the central part of a single moiré pattern, two hole-cylinder patterns precisely overlap, giving rise to a relatively low pattern density. The farther from the center of the hexagon, the more isolated overlapped motifs become, generating higher pattern density. Magnified SEM images and AFM height profiles further confirm that individual gold hole-cylinders in the superlattice array have a high aspect ratio ($h/w \approx 30$) and extremely small wall size (10 nm) (Figure 2b). In Figure 2c we show a photograph of the moiré pattern fabricated on a flexible PET film substrate. As the SSL technique enables fabrication of robust pattern arrays having high adhesion to the substrate, the fabrication of a complex superstructure on a flexible polymer substrate is realized. Due to the high aspect ratio of the gold nano pattern, our moiré superstructure is highly optically transparent (≈75%), in spite of the high density of complex superstructures.

As moiré fringes are highly sensitive to the misorientation angle between the superimposed layers,[23] a wide assortment of complex superstructures can be easily fabricated from a single pre-pattern simply by varying the misorientation angle (**Figure 3**). Figures 3a–f show various moiré superlattice structures generated from six different misorientation angles (20°, 14°, 10°, 8°, 5°, and 1°). As the misorientation angle decreases from 20° to 1°, the FFTs exhibit more regular six-fold symmetry (inset, top-right of Figure 3a–f). In particular, for θ = 20°, a complex aperiodic pattern resembling a 2D quasi-crystalline array was fabricated. This array exhibits almost 12-fold symmetry, which is incommensurate with the typical order of a moiré pattern. The corresponding periodicities in the moiré superstructures of Figure 3a–f are measured as 3, 4.9, 6.4, 7.5, 16.6, and 45 μm, respectively. Accordingly, moiré patterns with feature dimensions in the range of ≈3 μm to ≈40 μm can be fabricated by changing the misorientation angle from $\theta = 1°$ to $\theta = 20°$. The experimental measurements of the periodicities of the moiré patterns are in good agreement with the value calculated by the elementary superlattice theory (calculated data and graph is shown in Supporting Information Figure S2). In fact, the periodicity of the hexagonal moiré pattern is well described by the Rayleigh relation, $D = d/[2\sin(\theta/2)]$,[24] in

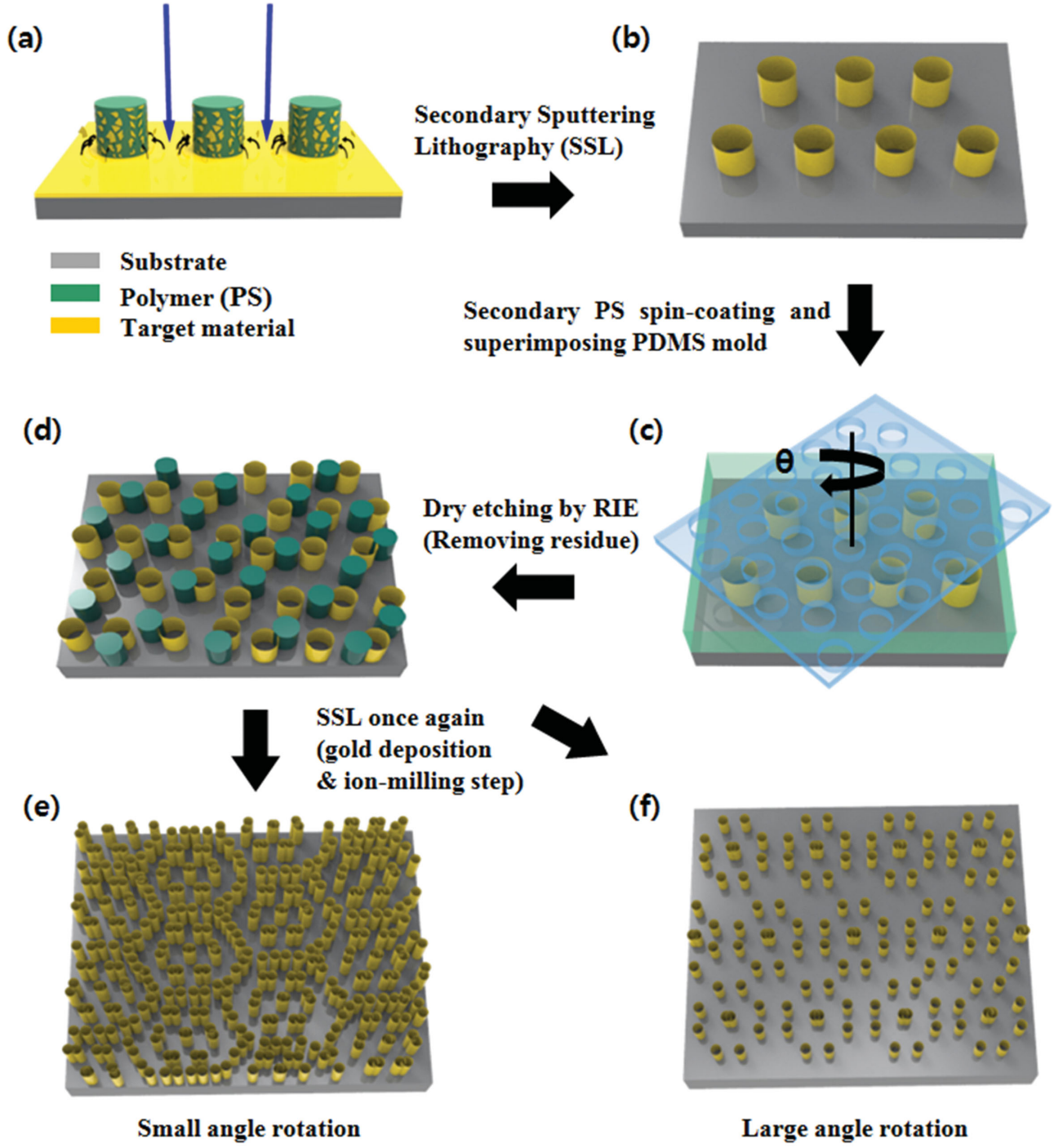

Figure 1. Schematic illustration showing the fabrication of a high aspect ratio moiré superlattice structure. a) The gold particles of the bottom gold layer (25 nm) were etched and emitted to the side surface of PS pre-patterns with a wide angle distribution, via the secondary sputtering phenomenon. b) The resulting patterned substrate was spin-coated with a thick layer of PS. c) A PDMS mold with the same lattice constant was pressed onto the PS surface at various misorientation angles. d) Using RIE the residue is removed and the secondary SSL process is then repeated. e,f) According to the rotation angle, various superstructures are fabricated.

which the periodicity (D) of the moiré pattern depends on the lattice constant (d) of a single motif and the misorientation angle (θ). As a single element of the superlattice is hexagonally organized, the Rayleigh relation is valid only when $0° < \theta \leq 30°$, and when the angular periodicity in the moiré pattern is 60°. For example, for the misorientation angles $\theta = 10°$, 50° (=60 – 10), and 70° (=60 + 10), the periodicity (D) is estimated to be ≈6 μm. In addition, if the misorientation angle is equal to multiples of the hexagonal periodicity (60°), the superimposed motifs exhibit no distinct angular difference. Therefore,

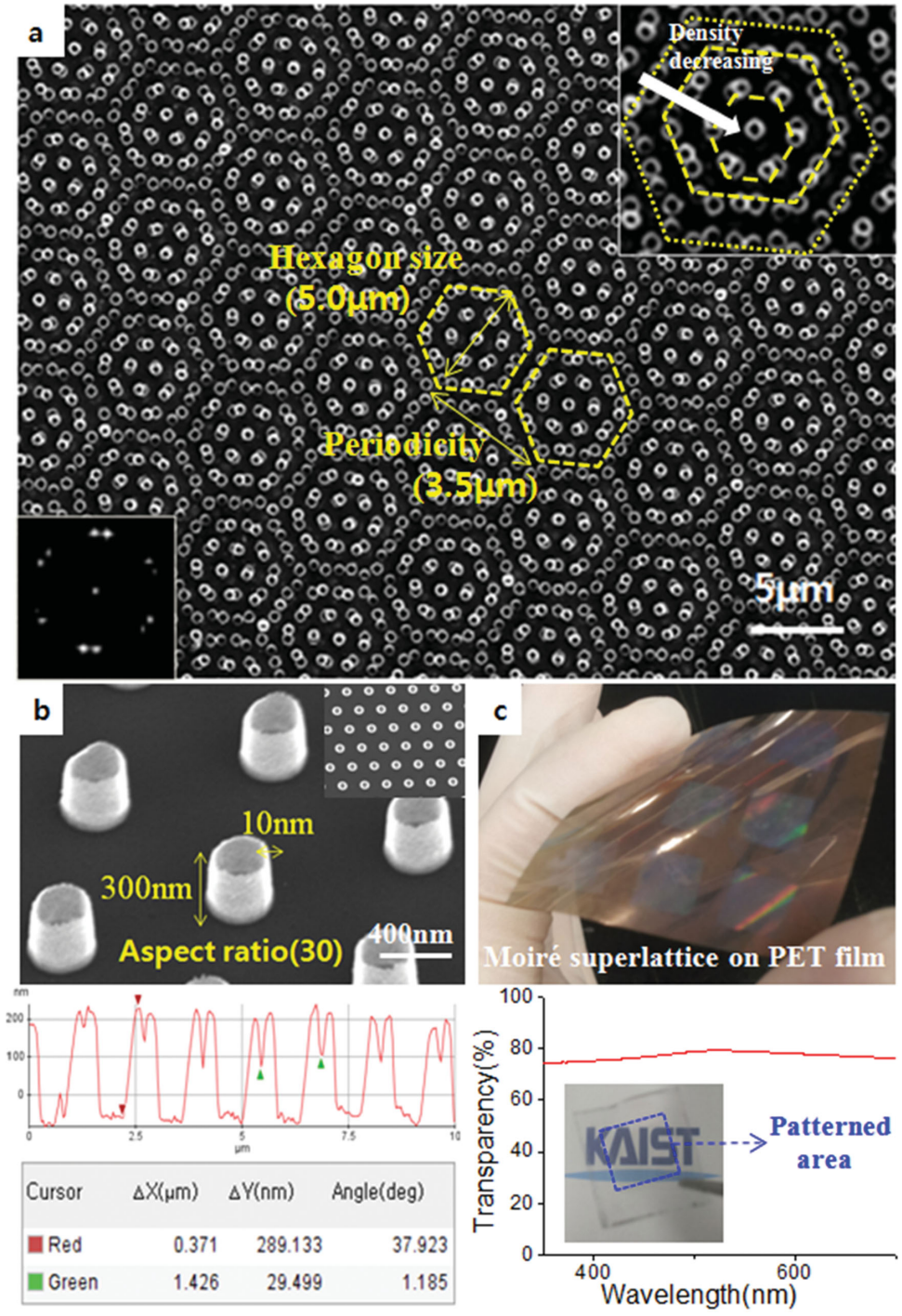

Figure 2. a) SEM image of a representative moiré superlattice structure. The periodicity of the superlattice is 3.5 μm, and the size of each moiré hexagon is 5 μm. The inset on the top-right shows decreasing density of the patterned area, and the inset on the bottom-left shows the FFT pattern of the SEM image. b) SEM image of a representative single SSL array. Nano hole-cylinders are highly organized into the hexagonal superlattice. AFM data confirm a high aspect ratio (≈30) and extremely small wall size (10 nm). c) Photo-image of the moiré superlattice fabricated on a flexible PET film. Due to the uniqueness of the SSL pattern, the superstructure shows high optical transparency (≈75%) (bottom graph).

the precisely overlapped hexagonal array of the SSL pattern can be generated from superimposed patterns, if the position of the second pattern is well-controlled with respect to the first set of hexagonal motifs (see Supporting Information, Figure S3).

We found that our complex moiré superlattice structures with high aspect ratio are very useful for highly selective liquid trapping with super-periodicity. **Figure 4**a,b illustrates an optical microscope image and a possible mechanism for liquid trapping on the moiré superlattice structure. Once the

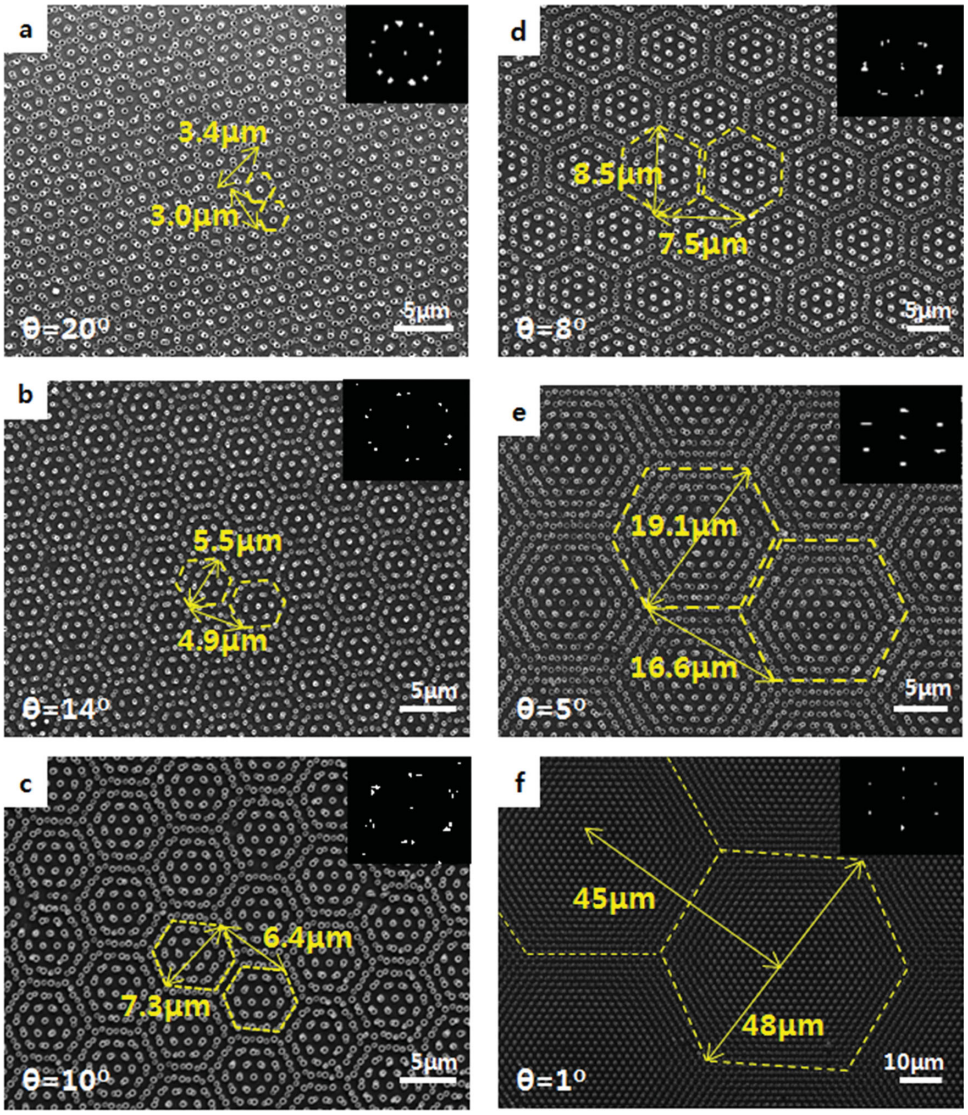

Figure 3. SEM images of various complex moiré superlattice structures. The superlattices are formed with a misorientation angle of a) 20°, b) 14°, c) 10°, d) 8°, e) 5°, and f) 1°. The FFTs of the moiré patterns are shown in the insets (top-right of each figure). The yellow hexagonal dashed line indicates the periodicity and size of the moiré hexagon. Based on the elementary theory of the moiré fringe, as the rotation angle decreases (20° → 1°), the periodicity of the superlattice increases (3 μm → 45 μm).

three-phase line of water began to shrink (corresponding to the flow of water from left (A) to right (C)), the unique optical images formed by the diffraction of light within the thin film of water could be observed (region B in Figure 4a,b). Consecutive snapshots of this process are shown in Figure 4c. After ≈1.0 s of evaporation, the water films are densely confined within the core region of the hexagonal moiré pattern. Considering Bragg's law ($n\lambda = 2d\ \sin\theta$) with a wavelength of visible light, it is expected that the liquid was densely and regularly confined within each moiré hexagon, creating a periodic liquid droplet superlattice on the surface (Figure 4d–f). The confined water within each moiré hexagon has about ≈300 nm thickness calculated by Bragg's low, showing a long-range order of hexagonal periodicity. This is a consequence of the fact that the moiré variation in pattern density of the gold hole-cylinder structure with a high aspect ratio has a strong effect on the pinning forces of the liquid on the pattern, resulting locally tuned wettability of patterned surfaces.

In order to further verify the periodic liquid trapping behavior, we implemented a controllable boundary confinement of commercial ink solution (water mixed with black ink) on the superlattice substrate. **Figure 5**a shows optical microscope images of a moiré superlattice structure before (left of image) and after (right of image) the application of ink solution. It is apparent that the black ink solution was trapped only in the central region of the hexagonal moiré superlattice. For both large (≈10 μm) and small (≈5 μm) hexagonal moiré superlattices, the ink solutions were trapped only in the central region of the hexagon. As this unique superlattice structure has a high aspect ratio, strong capillary forces acting on the liquid might be present in each hole-cylinder pattern, enabling intensive trapping of the ink solution (see Supporting Information,

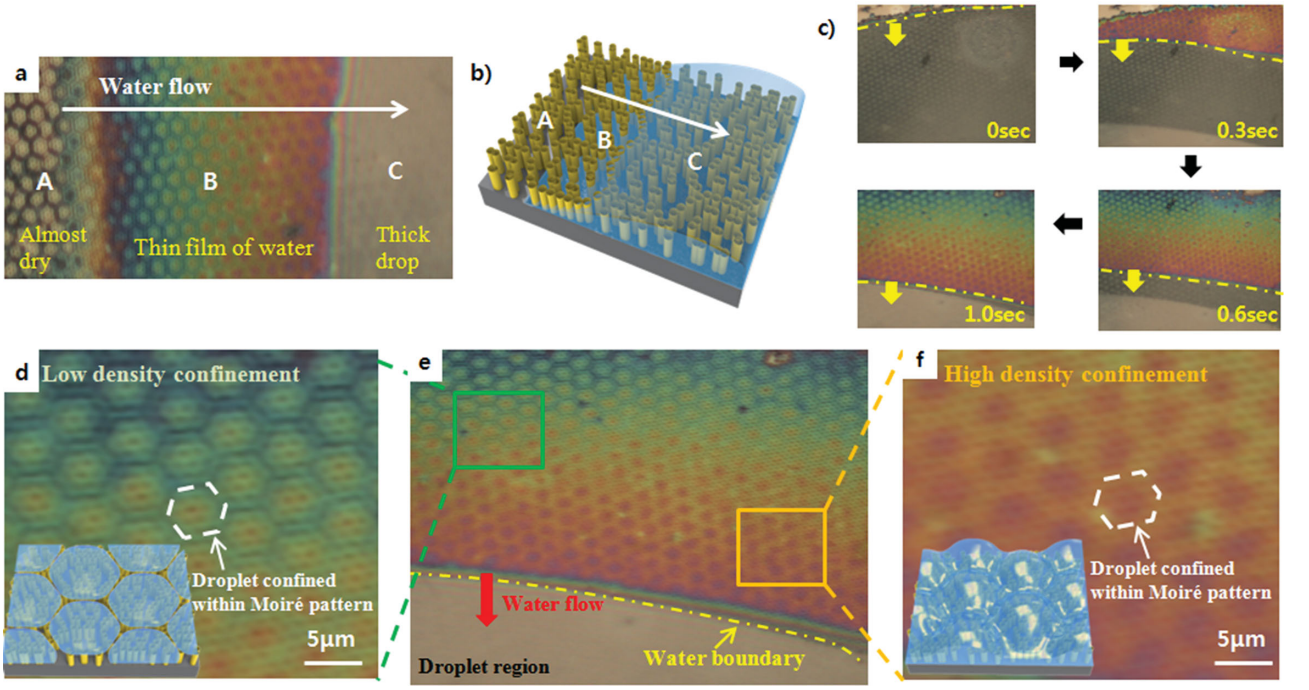

Figure 4. a,c–f) Optical microscope images of the evaporation procedure on a high aspect ratio moiré superlattice structure and b) schematic of the flow of a water droplet on the patterned surface. a) A thick droplet of water flows on the "C" region. The 'A' region is almost dry. The intermediate region B shows diffracted light, indicating the confinement of water. c) Snapshots of the evaporation process (clockwise from top-left image). e) With an enlarged image, a hexagonally organized confined liquid droplet is clearly seen behind the evaporation line. d) At the bluish region, a thin layer of water is confined and f) at the reddish region, a thick layer of water is confined within the hexagonal moiré patterns.

Figure S5). However, because the area specific density of the superlattice is significantly different between the central and edge regions of each moiré hexagon, the strength of the applied capillary forces is also different. This implies that the ink solution can be trapped within each moiré hexagon due to difference of hydrophobicity derived from specific density of the moiré patterns and finally selectively trapped in central part of the gold hole-cylinder pattern (right image of Figure 5b). Therefore, the ink solution was not trapped at the edge of the moiré hexagon (left image of Figure 5b). As a result, it is expected that by varying the periodicity of the moiré superlattice by simple modulation of the misorientation angles, control of the liquid trapping site can be achieved.

Using this unique property, we successfully demonstrate hierarchical nanoparticles (QDs) ordering with tunable super-periodicity into selective area of moiré superlattice by just solution-casting of toluene based QD solution on patterned surfaces. Delivering of nanoparticles or other solution-processed nanomaterials into user-defined array is a hard challenging area that applied to various research fields of basic science and technology.[25] For example, by delivering the bio-markers into a several square micrometers of hot-spot structure in which electromagnetic energy is concentrating, the superior plasmonic imaging application can be performed.[26] **Figure 6**a–c shows confocal microscope image of hierarchically ordered QDs superlattice with tunable super-periodicity from submicro to ≈20 micrometer scale. Left column of figure shows confocal scanning images and right column of figure shows combined image of optical microscope images and confocal scanning images. SEM images (inset, top-right of Figure 6a–c) show original moiré superlattice template for each QD ordering experiments. The combined images demonstrate that QD particles are only trapped in core parts of each moiré hexagon following super-periodicity of superlattice structure and not trapped in edge parts of each hexagon. With varying the periodicity of moiré superlattice structure by modification of misorientation angles, we easily modulate the alignment shape and super-periodicity. It is important to note that various kinds of nano-micro sized solution-processed particles can be easily ordered in moiré superlattice structure by just changing casted solution.

3. Conclusion

In conclusion, we have developed a new approach for the construction of complex superlattice structures with versatile super-periodicity using moiré fringe and secondary sputtering phenomenon. Wide assortments of high aspect ratio complex superstructures having different features on a 10 nm scaled wall were easily fabricated from simple starting components. In addition, as a result of the unique combination of the moiré fringe and SSL hole-cylinder pattern, we observed a novel micro-hydrodynamic phenomenon: Liquid is selectively trapped during evaporation on the patterned surfaces, a process dependent on the periodicity of the moiré superlattice structure. Using this phenomenon, we can selectively and hierarchically confine target materials within the moiré superlattice. Our observation is expected to elucidate the key morphological

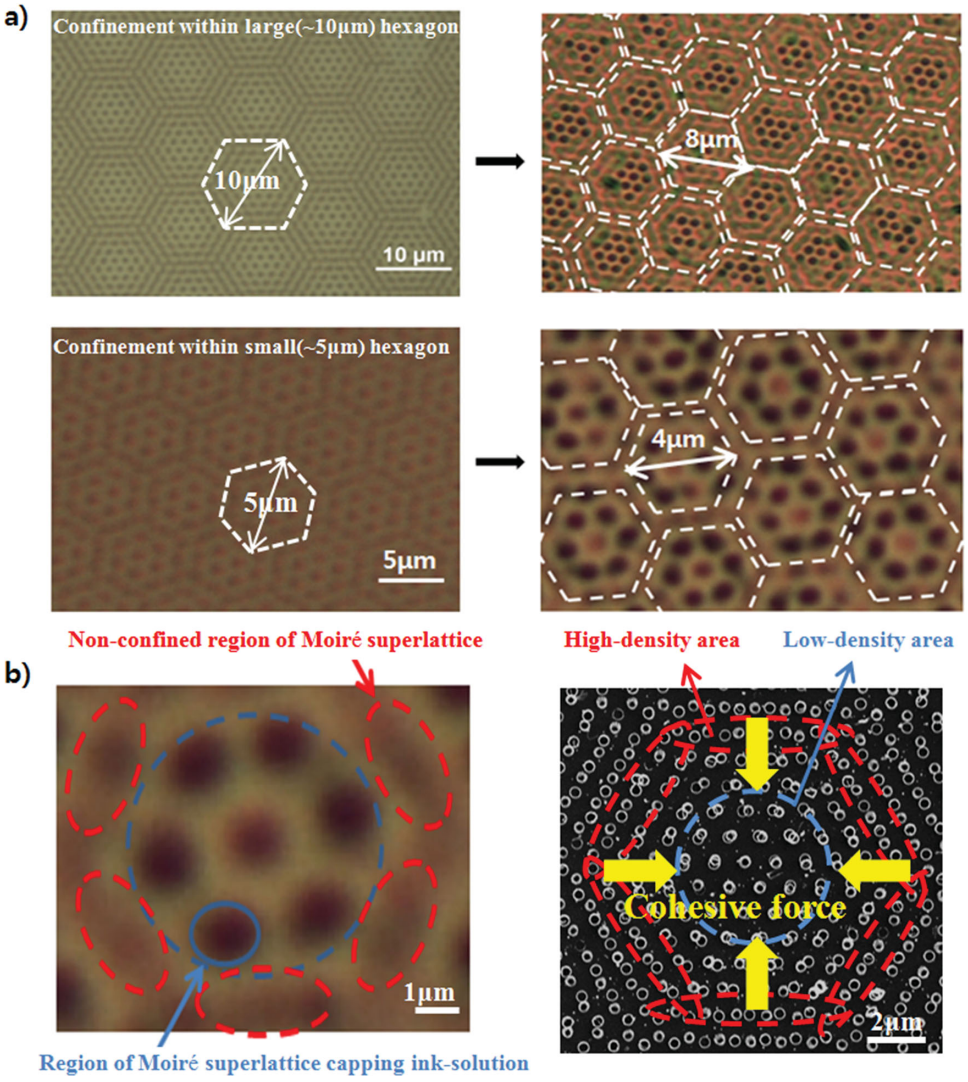

Figure 5. a) Optical microscope images of a hexagonally confined solution within a moiré superlattice structure, indicating super-periodicity. Due to the unique wetting property of the complex moiré pattern, solutions tend to be confined within the central part of each hexagon regardless of the size of the hexagon. b) Captured molecules within 3D hole-cylinder patterns are clearly shown (optical microscope image, left). Due to the high density of the SSL pattern in the edge area, difference of hydrophobicity is induced. The cohesive force on the liquid droplet is applied to the central part, which has a low pattern density (SEM image, right).

factors that govern the physics of liquid behavior on a complex patterned substrate. Accordingly, in the near future, this facile approach for complex superlattice structure could be used as optical substrate for imaging applications and open interesting perspectives in the assembly processes and the handling of the nano-micro size particles.

4. Experimental Section

Fabrication of Moiré Pattern: We used a silicon master mold consisting of a hexagonally patterned array of cylindrical posts, each being 400 nm in diameter and with 1000 nm of spacing. The entire area of the pattern was 10 mm × 10 mm. To realize secondary sputtering, a thin polystyrene (PS) film (2 wt% of PS (molecular weight = 18 000 g mol^{-1}) in anhydrous toluene) was spin-coated onto a glass substrate. Then, the poly(dimethylsiloxane) (PDMS) mold (Sylgard 184, Dow Corning; 10:1 ratio of prepolymer to curing agent) was pressed onto the PS spin-coated surface and heated above the glass transition temperature (135 °C) in a vacuum oven in order to drive the PS polymer into the void spaces of the mold pattern by capillary forces. The fabricated PS pattern array on the substrate was subsequently removed under low vacuum O_2/CF_4 RIE (40/60 sccm, pressure: 20 mTorr, RF power: 80 W). Following that, Au was deposited on the array by a thermal evaporation process, up to 25 nm layer thickness. An ion-milling process with Ar^+ gas was then applied to the pre-patterned surface sputtering pre-deposited Au layer. Finally, O_2 RIE (100 sccm, pressure: 20 mTorr) was used to remove the core PS polymer, resulting in the SSL pattern array. To make the moiré superlattice structure, polystyrene (PS) film at a high concentration (8 wt% of PS (molecular weight = 18 000 g mol^{-1}) in anhydrous toluene) was again spin-coated onto the fabricated hexagonal SSL pattern array with ≈400 nm film thickness, and the same PDMS mold was pressed onto the surface at various misorientation angles. This embossing process was done on a hot plate (155 °C), and, by repeating the same SSL procedure, a moiré superlattice structure consisting of gold hole-cylinder patterns can be obtained. To fabricate flexible superlattice

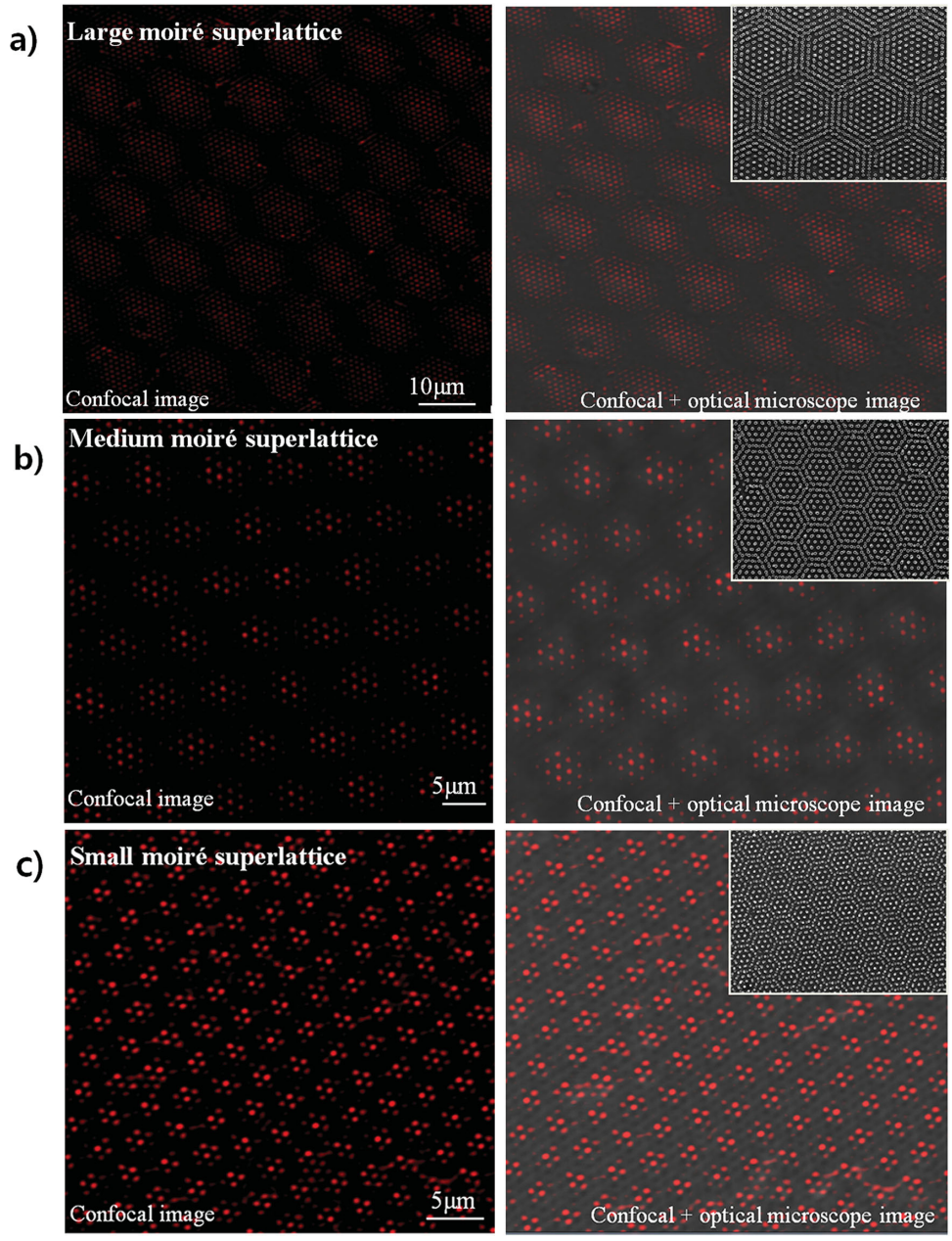

Figure 6. a–c) Confocal microscope image of a hierarchically ordered quantum dots (QDs) superlattice within the moiré superstructure. Insets (top-right) show the SEM image of each moiré superlattice structure. Regardless of the periodicity of the moiré pattern (sub-μm to 20 μm), the target nano-materials (QDs) are highly organized in the central parts of the moiré superstructure following super-periodicities of original moiré templates.

array, 5 cm × 5 cm PET film attached to Si wafer is used as substrate. Same procedure for secondary sputtering and moiré fringe technique is followed.

Liquid Confinement: A patterned glass substrate was placed on an optical microscope and 20μL of distilled water was placed on the moiré patterns. The entire evaporation procedure was then recorded. In order to elucidate the exact mechanism of self-assembly of the water droplets, 20 μL of distilled water mixed with black pen ink (monami153, Korea) was placed on the moiré patterns. After evaporation, core assembled structures were observed.

Quantum Dots Ordering within Moiré Superlattice Structures: CdS-ZnSe core–shell structure QDs were purchased from QD solution in a 15 mg mL^{-1} toluene-based solution (λ_{ab} = 578 nm, λ_{ex} = 594 nm). The QD solution was further diluted with toluene to a concentration of 1 mg mL^{-1}. A patterned glass substrate was spin-coated with 100 μL of this toluene based QD solution. After spin-coating process, patterned substrate is dried in room temperature for 20 min. With confocal microscope (LMS510 META NLO, Carl Zeiss), fluorescence image of QD ordering is obtained. To observe the fluorescence signals from the QDs with an excitation wavelength of 578 nm, a 543 nm HeNe laser was used as the input source with a BP 565–615 filter at 80% power.

Characterization: SEM (Sirion FE-SEM, FEI) was used to obtain images and to confirm the composition of materials. The incident energy of the electron beam was between 1 and 10 kV. The evaporation procedure and droplet structure were observed using an optical

microscope (OM) (LV-100POL, Nikon) equipped with a charge-coupled device (CCD) camera.

Supporting Information

Supporting Information is available from the Wiley Online Library or from the author.

Acknowledgements

S.-Y.C. and H.-J.J. contributed equally to this work. This research was supported by a National Research Foundation of Korea (NRF) grant funded by the Ministry of Science, ICT and Future Planning, Korea (MSIP, NRF-2012R1A2A1A01003537).

Received: June 16, 2014
Revised: July 18, 2014
Published online: September 1, 2014

[1] J. H. Mun, Y. H. Chang, D. O. Shin, J. M. Yoon, D. S. Choi, K.-M. Lee, J. Y. Kim, S. K. Cha, J. Y. Lee, J.-R. Jeong, Y.-H. Kim, S. O. Kim, *Nano Lett.* **2013**, *13*, 5720–5726.
[2] D. O. Shin, J. H. Mun, G.-T. Hwang, J. M. Yoon, J. Y. Kim, J. M. Yun, Y.-B. Yang, Y. Oh, J. Y. Lee, J. Shin, K. J. Lee, S. Park, J. U. Kim, S. O. Kim, *ACS Nano* **2013**, *7*, 8899–8907.
[3] D. O. Shin, D. H. Lee, H.-S. Moon, S.-J. Jeong, J. Y. Kim, J. H. Mun, H. Cho, S. Park, S. O. Kim, *Adv. Funct. Mater.* **2011**, *21*, 250–254.
[4] V. Luchnikov, A. Kondyurin, P. Formanek, H. Lichte, M. Stamm, *Nano Lett.* **2007**, *7*, 3628.
[5] Y. He, S. H. Ko, Y. Tian, A. E. Ribbe, C. Mao, *Small* **2008**, *4*, 1329.
[6] T. Hirai, S. Hayashi, *Colloids Surf. A: Physiochem. Eng. Aspects* **1999**, *153*, 503.
[7] A. Reinmüller, H. J. Schöpe, T. Palberg, *Soft Matter* **2010**, *6*, 5312.
[8] S. H. Kang, N. Wu, A. Grinthal, J. Aizenberg, *Phys. Rev. Lett.* **2011**, *107*, 177802.
[9] A. Singh, C. Dickinson, K. M. Ryan, *ACS Nano* **2012**, *6*, 3339.
[10] S. M. Lubin, A. J. Hryn, M. D. Huntington, C. J. Engel, T. W. Odom, *ACS Nano* **2013**, *7*, 11035.
[11] S. Balci, A. Kocabas, C. Kocabas, A. Aydinli, *Appl. Phys. Lett.* **2011**, *98*, 031101.
[12] L. Fernández, M. Corso, F. Schiller, M. Ilyn, M. Holder, J. E. Ortega, *Appl. Phys. Lett.* **2010**, *96*, 013107.
[13] J. Mao, H. Zhang, Y. Jiang, Y. Pan, M. Gao, W. Xiao, H.-J. Gao, *J. Am. Chem. Soc.* **2009**, *131*, 14136.
[14] R. A. Wind, M. J. Murtagh, F. Mei, Y. Wang, M. A. Hines, S. L. Sass, *Appl. Phys. Lett.* **2001**, *78*, 2205.
[15] J. Choi, R. B. Wehrspohn, U. Gösele, *Adv. Mater.* **2003**, *15*, 1531.
[16] B. Chen, K. Lu, *Langmuir* **2011**, *27*, 4117.
[17] C. J. Kloxin, T. F. Scott, H.-Y. Park, C. N. Bowman, *Adv. Mater.* **2011**, *23*, 1977.
[18] S. M. Lubin, W. Zhou, A. J. Hryn, M. D. Huntington, T. W. Odom, *Nano Lett.* **2012**, *12*, 4948.
[19] H.-J. Jeon, K. H. Kim, Y.-K. Baek, D. W. Kim, H.-T. Jung, *Nano Lett.* **2010**, *10*, 3604.
[20] H. S. Jeong, H.-J. Jeon, Y. H. Kim, M. B. Oh, P. Kumar, S.-W. Kang, H.-T. Jung, *NPG Asia Mater.* **2012**, *4*, e7.
[21] J.-S. Kim, H.-J. Jeon, H.-W. Yoo, Y.-K. Baek, K. H. Kim, D. W. Kim, H.-T. Jung, *Adv. Funct. Mater.* **2014**, *24*, 841.
[22] H.-J. Jeon, H. S. Jeong, Y. H. Kim, W.-B. Jeong, J. Y. Kim, H.-T. Jung, *ACS Nano* **2014**, *8*, 1204.
[23] I. Amidror, *The Theory of the Moiré Phenomenon, Vol. 1: Periodic Layers*, Kluwer Academic, Dordrecht, **2000**.
[24] G. Oster, C. Zwerling, M. Wasserman, *J. Opt. Soc. Am.* **1964**, *54*, 169.
[25] E. Miele, M. Malerba, M. Diapalo, E. Rondanina, A. Toma, F. D. Angelis, *Adv. Mater.* **2014**, *26*, 4179.
[26] F. De. Angelis, F. Gentile, F. Mecarini, G. Das, M. Moretti, P. Candelro, M. L. Coluccio, G. Cojoc, A. Accardo, C. Liberale, R. P. Zaccaria, G. Perozziello, L. Tirinato, A. Toma, G. Cuda, R. Cingolani, E. D. Fabrizio, *Nat. Photonics* **2011**, *5*, 682.